

# Reachability Analysis for Pursuer-Evader Dynamic Games

Apoorva Banerjee and Reuben Georgi

## Abstract

This report examines the existence of backward reachable sets for dynamic games involving a superior evader and three or more identical & inferior pursuers. The reachable sets are computed by numerically solving the Hamilton-Jacobi-Isaacs (HJI) partial differential equation (PDE) and the initial interception set is defined using the concept of the Apollonius-circle. The effects of changing the number of pursuers and the relative speed ratio on the reachable sets are then explored.

## I. INTRODUCTION

Pursuit-evasion dynamic games have been the subject of a considerable amount of research due to its relevance in a wide of range of applications which includes control and guidance of unmanned vehicles, defense systems and robotic systems. One of the topics introduced in this course was the concept of reachability and it had been motivated by considering the Two Aircraft Conflict Resolution problem. It helped to demonstrate how the computation of reachable sets enables the synthesis of safe controllers by determining the sets of states from which the system may reach an unsafe configuration. From this, it is clear how reachability analysis can be a beneficial tool in the study of pursuit-evasion dynamic games.

In the effort to learn more about reachability analysis, Gillula et al. [1] proved to be a good starting point as it provided some brief background on the Hamilton-Jacobi formulation of reachability in the context of practical applications that they were trying to implement. It provides an overview on how a solution to the reachability problem can be obtained by defining the boundary of the initial set as the zero-level set of an appropriately selected cost function and also further explains how the optimal value of the cost function can be found using dynamic programming. This brief introduction enabled us to better understand [4] which first demonstrated that the viscosity solution of a particular time-dependent HJI PDE provides an implicit surface representation of the continuous backwards reachable set. The paper goes on to describe an algorithm which makes use of level set literature for computing the set of reachable states of a continuous dynamic game. It is this algorithm which was implemented in the Level Set Toolbox [3], which is used for the numerical computation of reachable sets in this project.

Gillula et al. [1] also uses the toolbox in order to guarantee the safety and performance of robotic aerial vehicles for two distinct applications. In the first application, it is used to verify the safety and performance criteria for an aerobatic UAV maneuver (specifically, a backflip maneuver). This involves generating a backwards reachable set for the final maneuver by starting from the final or target set, and this is called the capture set for the maneuver. This process can be repeated for the preceding maneuvers to identify a suitable sequence to perform the required task. In the second application, reachable sets are used to address the task of collision avoidance between multiple UAVs and it is more concerned with the property of safety. This involves using a switched control approach to take action when the calculated avoid sets of the agents are too close to each other. The first application is relevant to the current topic as it deals with the concept of attainability in which the desired goal of the controller is to drive the system into some desired set by minimizing the cost function, in the presence of disturbances which attempt to drive the system away.

Having gained some insights from [1] about reachable set analysis, Altafer et al.[2] focuses on the guidance of missiles using this technique and also uses the Level Set Toolbox. However, their work is relevant to any

dynamic game involving lower-speed pursuers attempting to intercept a superior evader and the main aim of this project is to explore and expand on this work. Another take way from this paper is the terminal path constraint or the final value function of the HJI which makes use of the concept of the Apollonius circle to define a perfectly encircled formation of the pursuers around the missile. This concept is explained in greater detail in [5] which uses the idea of Apollonius circles to develop an escape strategy for a high speed evader from multiple pursuers.

## II. PROBLEM FORMULATION

### A. Cost Function

The aim is to find the reachable sets for a multi-player pursuit-evasion differential game using optimal control methods by defining a suitable cost function of the form,

$$J = \phi(X, t_f) + \int_{t_0}^{t_f} L(X, a, b_1, b_2, \dots, b_n, t) dt$$

Here,  $\phi(X, t_f)$  is called the terminal cost function, while  $\int_{t_0}^{t_f} L(X, a, b_1, b_2, \dots, b_n, t) dt$  is called the path cost and  $X$  represents the state vector. Here,  $a$  represents the evader's control input, while  $b_1, b_2, \dots, b_n$  represent the input from the disturbance, which refers to the pursuer's control input.

### B. System Dynamics

In the considered problem, the evader is of superior quality as compared to the pursuer, and hence that opens up an interesting discussion about the possible reachable sets that can be generated through the solution of the Hamilton-Jacobi-Isaac PDE. The HJI Partial Differential Equation is described as follows:

Consider a dynamical system,

$$\begin{aligned} \dot{x} &= f(x(t), u(t), d(t)) \\ x(0) &\in X_0 \text{ ( or } x(t_f) \in Y_0 \text{ ) for } t \in [t_0, t_f] \end{aligned}$$

Additionally, we also have  $0 \leq t_f \leq \infty$ ,  $x \in R^n$

$u \in U \subset R^m$  is the control input

$d \in D \subset R^p$  is the disturbance input

Also,  $X_0$  and  $Y_0$  represent the initial and target sets, respectively.

$X_0 = \{x : l(x) < 0\}$  and  $Y_0 = \{x : y(x) \leq 0\}$

The Hamilton-Jacobi-Isaacs formulation is used to solve differential games using optimal control techniques. The terminal cost function value of the objective functional is given by:

$$V(X) = \inf_{b_j \in U^p} \sup_{a \in U^e} J(X, a, b_1, b_2, \dots, b_n, t)$$

The solution of the time-dependent HJI PDEs gives us the following two equations:

$$\frac{\partial V(X, t)}{\partial t} + H(X, V_x, t) = 0$$

Subject to:  $V(X, t_f) = \phi_0(X, t_f)$

Here,  $H(\cdot)$  is the Hamiltonian and is given by:

$$H(X, V_x, t) = \max_{a \in U^e} \min_{b_j \in U^p} \frac{\partial V}{\partial X} f(X, a, b_1, \dots, b_n, t)$$

Here, this expression for the Hamiltonian suffices because the running cost, given by  $L(\cdot)$  is zero. These equations are solved backwards in time, such that the terminal cost  $\phi(X, 0) = \phi_0(X)$ . Solving these equations [brief outline given in III-B1] gives us the following optimal decisions for the evader and pursuer controls, respectively:

$$a^* = \arg \max_{a \in U^e} \min_{b_j \in U^p} \frac{\partial V(X, t)}{\partial X} f(X, a, b_1, b_2, \dots, b_n, t)$$

$$b_j^* = \arg \max_{a \in U^e} \min_{b_j \in U^p} \frac{\partial V(X, t)}{\partial X} f(X, a^*, b_1, b_2, \dots, b_n, t)$$

### III. SOLUTION APPROACH

#### A. Apollonius Circles

From [5], we understand that the Apollonius circle is the locus of points such that the ratio of distances to the evader and pursuer is equal to their speed ratio and the use of this concept in Pursuit Evader games was first discussed by Isaacs. It also describes how a perfectly encircled formation (PEF) is one in which a set of pursuers encircle an evader in such a way that the Apollonius circle of each pursuer will have common tangent points with its neighboring pursuers and all the tangent lines from the common tangent points pass through the evader. [2] also uses this concept to define its interception set and terminal function value.

In a pursuit-evasion game with three pursuers,  $p_1(x_1, y_1)$ ,  $p_2(x_2, y_2)$  and  $p_3(x_3, y_3)$  form three Apollonius circles with the following radius:

$$r_j = \frac{\alpha}{1 - \alpha^2} \sqrt{(x_{pj} - x_e)^2 + (y_{pj} - y_e)^2}$$

and centred at  $c_j = (\frac{x_{pj} - x_e \alpha^2}{1 - \alpha^2}, \frac{y_{pj} - y_e \alpha^2}{1 - \alpha^2})$ , where  $j = 1, 2, 3$  and  $\alpha = V_p/V_e < 1$ .

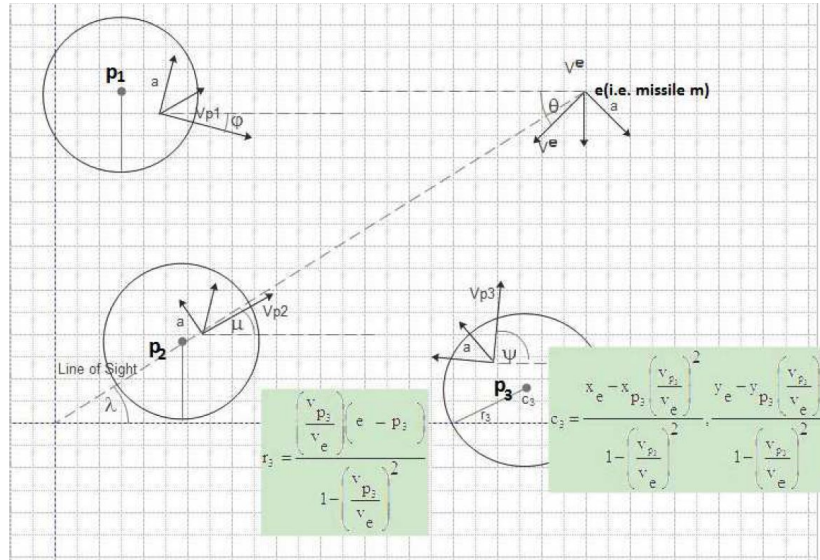


Fig. 1: Engagement Geometry in a One-Evader-Three-Pursuer scenario. Here  $a$  is the lateral acceleration [From Ref. 2 pp. 373]

From [5] and [2], we see that one of the conditions that define the interception set is when the pursuers' Apollonius circles radii approach distance  $\delta^j$  with the evader expressed mathematically as,

$$r_j = \frac{\alpha}{1 - \alpha^2} \sqrt{(x_{pj} - x_e)^2 + (y_{pj} - y_e)^2} \leq \delta^j$$

Another condition is that relative heading angles should be given by,  $\theta_{r_j} = j \frac{2\pi}{n}$  where  $j$  takes on values from 1 to  $n$  (number of pursuers). Note that at least 3 pursuers are needed to use the Apollonius circles formulation. Finally, as proved in [5], the speed of each pursuer required to create a perfectly encircled formation using  $N$  identical pursuers is  $\sin(\pi/N)$  times the speed of evader which can be expressed as  $\frac{V_p}{V_e} \geq \sin(\frac{180^\circ}{n})$ .

## B. Reachable Set Solution

1) *Mathematical Derivations:* The case of one evader and one pursuer is elaborated in this subsection. In this case, a superior evader seeks to prevent interception by a relatively inferior (or, slower) pursuer. Here, it is easier to analyze the system dynamics by placing the frame of reference on the evader, with its velocity vector facing along the positive x-axis. The relative dynamics of the system is given as follows:

$$\dot{x} = -V_e + V_p \cos \psi + ay \quad (1)$$

$$\dot{y} = V_p \sin \psi - ax \quad (2)$$

$$\dot{\psi} = b - a \quad (3)$$

Here,  $V_p$  and  $V_e$  are the speeds of the pursuer and evader, respectively, and are taken as constants. Also,  $a$  and  $b$  represent the turning rates of the evader and pursuer, respectively. Each of the turn rates has a maximum limit that can be specified while implementing the BRS analysis.

In order to find the optimal solution to the problem, we define the Hamiltonian as:

$$H = p^T \dot{X}$$

The control of the evader tries to maximise this function, while the disturbance control (control of the pursuer) is trying to minimize the same.

$$H^* = \max_{a \in A} \min_{b \in B} p^T \dot{X}$$

Here,  $p = [p_x \ p_y \ p_\psi]^T$  are known as the co-states, or Lagrange Multipliers. Expanding the terms, we obtain the Hamiltonian as:

$$H = p_x[-V_e + V_p \cos \psi + ay] + p_y[V_p \sin \psi - ax] + p_\psi[b - a]$$

Rearranging the equations by separating the terms of the control and disturbance, we get:

$$H = p_x[-V_e + V_p \cos \psi] + p_y[V_p \sin \psi] + [p_x y - p_y x - p_\psi]a + p_\psi b$$

Here, the next step would be to define the Euler-Lagrange Equations:

$$\dot{p}_i = -\frac{\partial H}{\partial X_i}$$

Using the equation, we obtain:

$$\dot{p}_x = ap_y \quad (4)$$

$$\dot{p}_y = -ap_x \quad (5)$$

$$\dot{p}_\psi = p_x V_p \sin \psi - p_y V_p \cos \psi \quad (6)$$

Given that the Hamiltonian is linearly varying with respect to the control and disturbance input, we can define the "Switching Functions" in terms of both inputs. The control law equations are given by:

$$\frac{\partial H}{\partial a} = p_x y - p_y x - p_\psi \quad (7)$$

$$\frac{\partial H}{\partial b} = p_\psi \quad (8)$$

In the case when the control input is for the optimal trajectory, we have:

$$a^* = \text{sign}[p_x y - p_y x - p_\psi]$$

$$b^* = \text{sign}[-p_\psi]$$

This is because, the control  $a$  (of the evader) tries to maximize the value function, while the control  $b$  (of the pursuer) tries to minimize the same. Similarly, the dynamics can be derived for multiple pursuers in the same way by using an evader centric frame of reference.

2) *One Evader and Multiple Pursuers*: As mentioned in [1], [2] and [3], there is an exponential increase in computational complexity as the number of dimensions increase and it is difficult to obtain the BRS directly for even a small number of pursuers through the toolbox.

It is then prudent to reduce the dimensionality of the problem and as noted in [2], a complex BRS analysis can be decomposed into several 1 Evader + 1 Pursuer subsystems, provided that the subsystems have no overlapping states with other subsystems. This reduces computational complexity, as the system is decomposed into several single-evader-pursuer subsystems.

$$\Gamma = \bigcup_{j=1}^n \Gamma_j \quad (9)$$

In this case,  $n = 3$ , and  $m = 3$  is the dimension of the state space in the case of the one evader-pursuer relative dynamics equations. The relative dynamics of the subsystem can be taken from Section III-B1.

### C. Level Set Toolbox

The Level Set Toolbox utilizes level set techniques by considering the reachable set to be the zero sub-level set of an appropriately-chosen function, and the boundary of this set is propagated under a nonlinear flow field using a validated numerical approximation of a time-dependent HJI Partial Differential Equation. The boundary of the backward reachable set is computed as the zero level set of the solution of the Hamilton-Jacobi partial differential equation on a grid representing a discretization of the state space.

Since using the toolbox was crucial to the project, a considerable amount of time was spent reading the user manual and exploring the various examples which were provided. Thus, it seems appropriate to briefly describe how the toolbox works and how it has been utilized here.

- The Level Set Toolbox uses a Cartesian grid to represent the reachable set over the state space, and consequently computational complexity grows exponentially in the number of dimensions. While setting up the grid in 3 dimensions is relatively straightforward, one aspect of note for this project was that the computational domain for  $\theta$  for each pursuer has to be defined appropriately to obtain the reachable sets for a PEF interception.
- Also related to the grid, boundary conditions (BCs) have to be appropriately set for the faces of the computational domain and the toolbox provides the option to set Dirichlet, Neumann, periodic or extrapolation boundary conditions. The domain for  $\theta$  uses a periodic BC whereas extrapolation BCs are used for the others.
- The initial conditions for this problem refers to the interception set for which the backward reachable set needs to be computed. As mentioned earlier, the interception set for this problem is defined by the pursuers' Apollonius circles radii approaching distance  $\delta^j$  with the evader. Thus, the initial condition is defined by a signed distance function representing a cylinder and its radius depend on the values considered for  $\alpha$  and  $\delta^j$ . The toolbox also provides the option to create implicit surface functions for other shapes such as spheres and rectangles.
- The toolbox solves the PDE using the method of lines by approximating the spatial terms (which in this case is the Hamiltonian) as a single function  $G(x, \phi(x, t))$  and then solving the differential equation,  $\frac{\partial \phi(x, t)}{\partial t} = G(x, \phi(x, t))$  point wise at each state  $x$ . The Hamiltonian is approximated using the Lax–Friedrichs method which is a numerical method for the solution of hyperbolic partial differential equations based on finite differences.
- The toolbox provides different options for Runge-Kutta (RK) integrators which solve the approximated differential equation and also provides options for the finite difference schemes used to approximate spatial derivative terms. These choices can affect the stability and accuracy of the solution.

#### IV. NUMERICAL RESULTS

In this section, we use the dynamics obtained in III-B1 in order to compute the BRS for the pursuit-evasion dynamic game, using the Level Set Toolbox by Mitchell [3]. The parameters for cases A and B are as follows:

$$V_p = 9m/s, V_e = 10m/s, \omega_e = \omega_p \in [-1, 1]$$

For Case C, the speed ratio is varied and  $V_p = 7.5m/s$  while the other parameters are kept the same. Here,  $V_p$  and  $\omega_p$  denote the speed and turn rate range of the pursuer, while  $V_e$  and  $\omega_e$  denote the same for the evader. Clearly, here the parameters of the evader are superior to the pursuer. The velocities were chosen such that  $\frac{V_p}{V_e} \geq \sin(\frac{180^\circ}{n})$  is satisfied. The interception set is defined by an Apollonius circle of radius  $r_j = \frac{\alpha}{1-\alpha^2} \sqrt{(x_{pj} - x_e)^2 + (y_{pj} - y_e)^2} \leq \delta^j = 3$ . It is to be noted that the pursuit-evasion game assumes perfect information, while the pursuers themselves use an open loop trajectory with non-cooperative and non-anticipative strategy. In the following sections, the results of three variations of the pursuer-evader dynamic game are presented.

##### A. One Evader and Three Pursuers (Base Case)

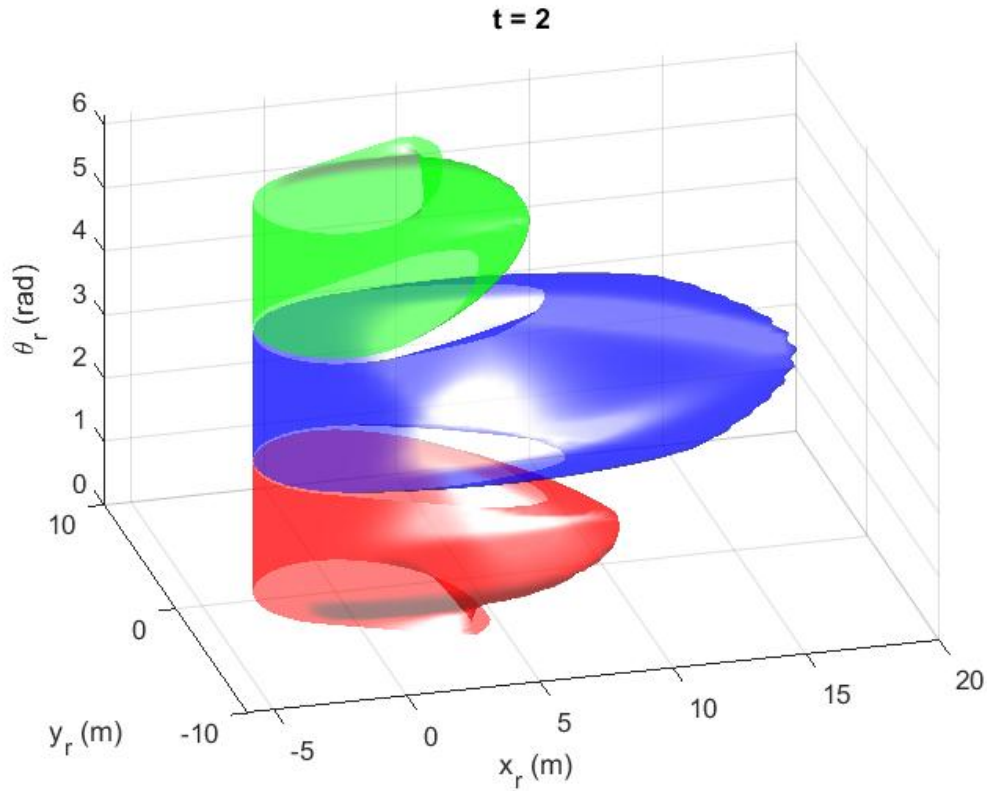


Fig. 2: Reachability Analysis for Three Pursuers and One Evader

Figure 2 shows the Backward Reachable Set (BRS) obtained for the one evader and three pursuers dynamic game. As the movement of the evader is along the x-axis based on our dynamics, the maximum reach is expected due to a pursuer which is in the opposite direction, with a relative angle of  $180^\circ$  with respect to the evader. This reachable subset is shown in blue, where  $\theta_{r2} \in [\frac{2\pi}{3}, \frac{4\pi}{3}]$  for the second pursuer and helps to serve as a sanity check.

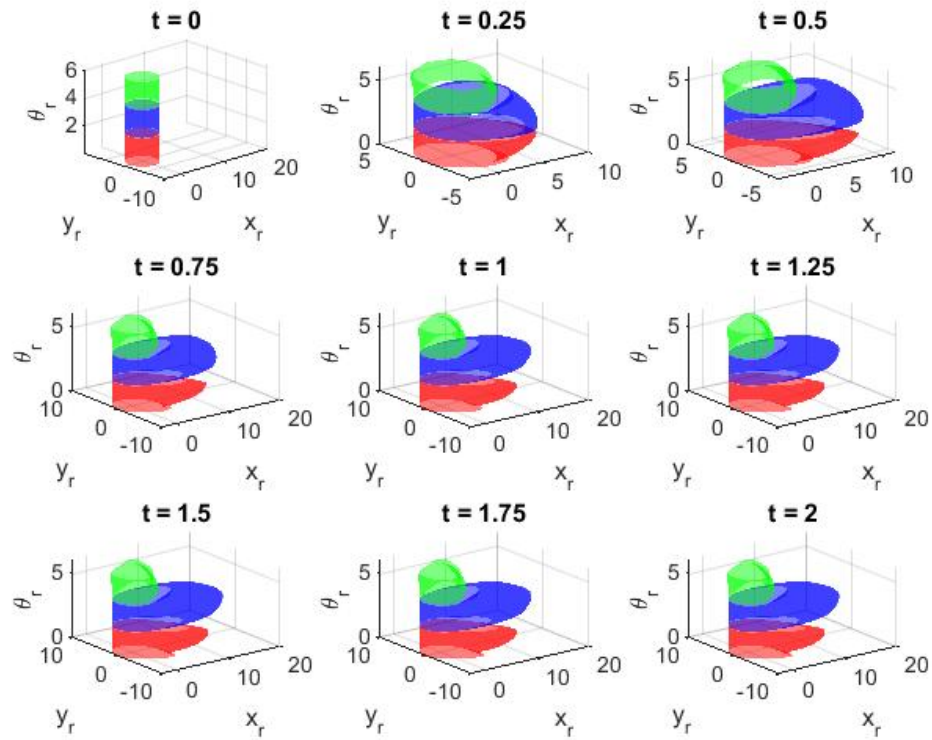


Fig. 3: Illustrating the growth of Backward Reachable Set from  $t = -2$  to  $t = 0$

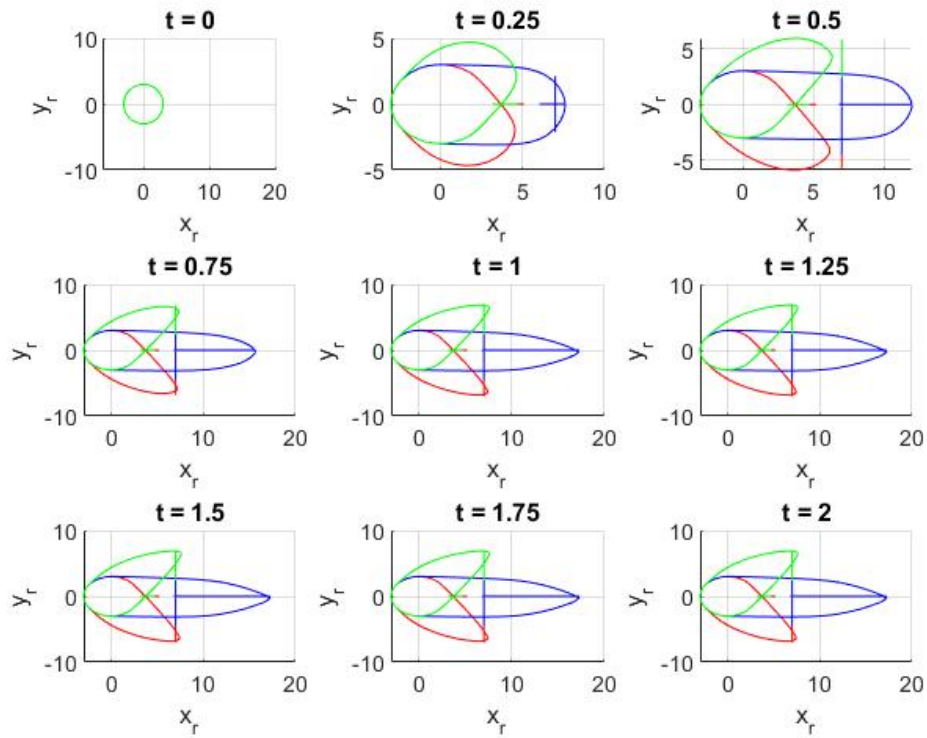


Fig. 4: 2D Contour Plot of Backward Reachable Set from  $t = -2$  to  $t = 0$



As mentioned when discussing the toolbox, the initial conditions were set up using the Level Set Toolbox with 3 cylinders centred at the origin with  $\delta^j = 3$ , where  $j = 1, 2, 3$ . Each cylinder represents the initial interception set with the evader for the range of angles assigned to each pursuer for a PEF interception. If an pursuer starts its motion from outside the corresponding reachable set in a finite time horizon, the evader has a guaranteed escape strategy.

Here, there are three separate cases of the relative heading  $\theta_{rj}$  taken, namely three disjoint intervals of  $[0, \frac{2\pi}{3})$ ,  $[\frac{2\pi}{3}, \frac{4\pi}{3})$  and  $[\frac{4\pi}{3}, 2\pi]$ . Their reachable sets are shown in red, blue and green, respectively. The three subsystems have no common overlapping states, and hence the decomposition of the three-pursuer system into three separate one-pursuer subsystems is valid. Starting from the interception set, it was observed that the Backward Reachable Set continues to grow, and stops close to  $t = -2$ . 2D contour plots of the reachable set diagrams are displayed in Figure 4, and it provides the sets of states from which the 3 inferior pursuers can form a PEF with the evader and capture it. The contours plots for the first, second and third pursuers (represented by red, blue and green respectively) are plotted for  $\theta_{r1} \approx 60^\circ$ ,  $\theta_{r2} \approx 180^\circ$  and  $\theta_{r3} \approx 300^\circ$  (in accordance with  $\theta_{rj} = j \frac{2\pi}{n}$ ) and thus this provides the backwards reachable set for one possible perfectly encircled formation.

### B. One Evader and Four Pursuers

As with the 3 pursuers case, the BRS analysis for four pursuers can also be carried out in the same way (as specified in Section III-B2). Here, the radius  $\delta^j = 3$  is as specified in the previous subsection. However, the values of  $\theta_{rj}$  would be divided into four subsets:  $[0, \frac{\pi}{2}]$ ,  $[\frac{\pi}{2}, \pi]$ ,  $[\pi, \frac{3\pi}{2}]$  and  $[\frac{3\pi}{2}, 2\pi]$ . As in the previous case, the reachable sets shaded blue and green include angles close to  $180^\circ$  and thus have the furthest reach which was the expected result. As before, the growth of reachable set and 2D contour plots are provided in figures 6 and 7. The contours plots in this case, represent a PEF with  $\theta_{r1} \approx 45^\circ$ ,  $\theta_{r2} \approx 135^\circ$ ,  $\theta_{r3} \approx 225^\circ$  and  $\theta_{r4} \approx 315^\circ$ . Based on the results from cases A and B, it appears that increasing the number of pursuers has decreased the size of the backwards reachable set.

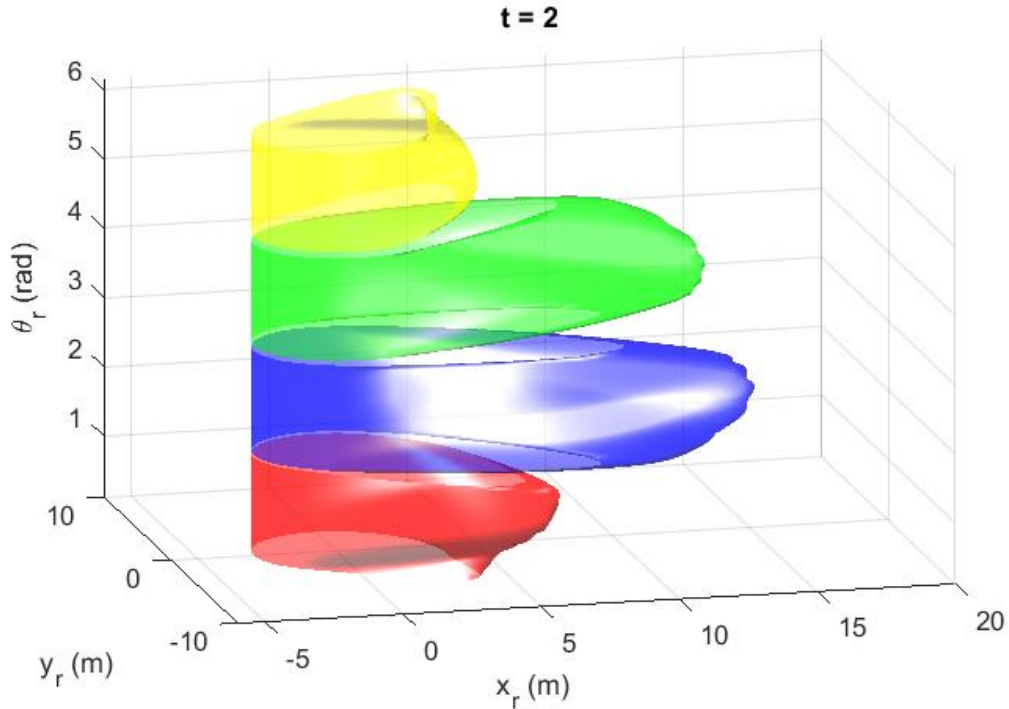


Fig. 5: Reachability Analysis for Four Pursuers and One Evader



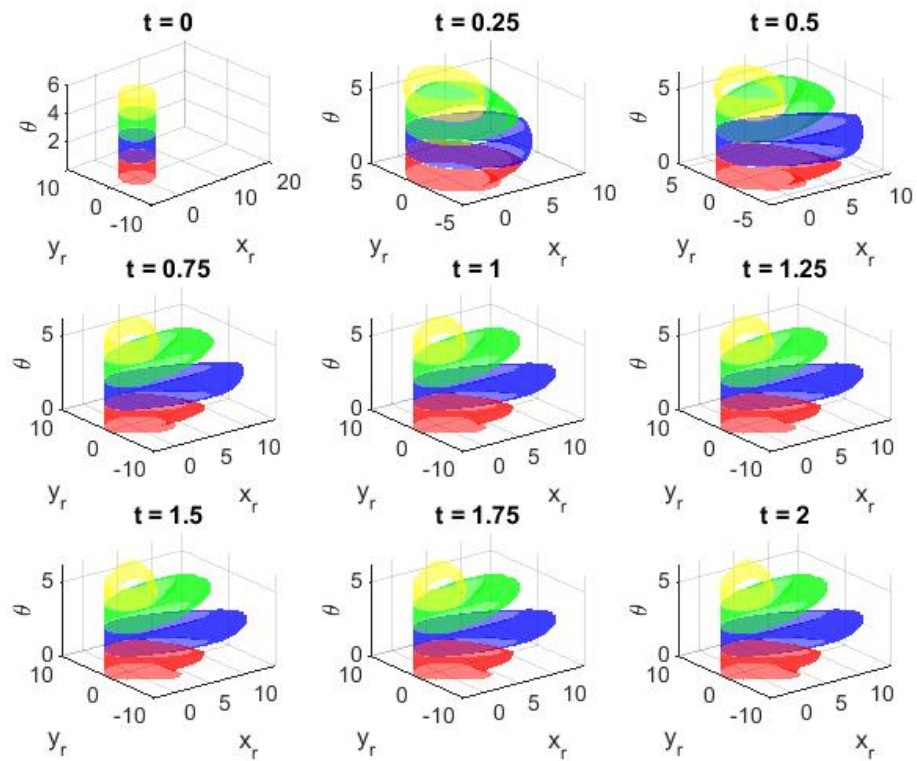


Fig. 6: Illustrating the growth of Backward Reachable Set from  $t = -2$  to  $t = 0$

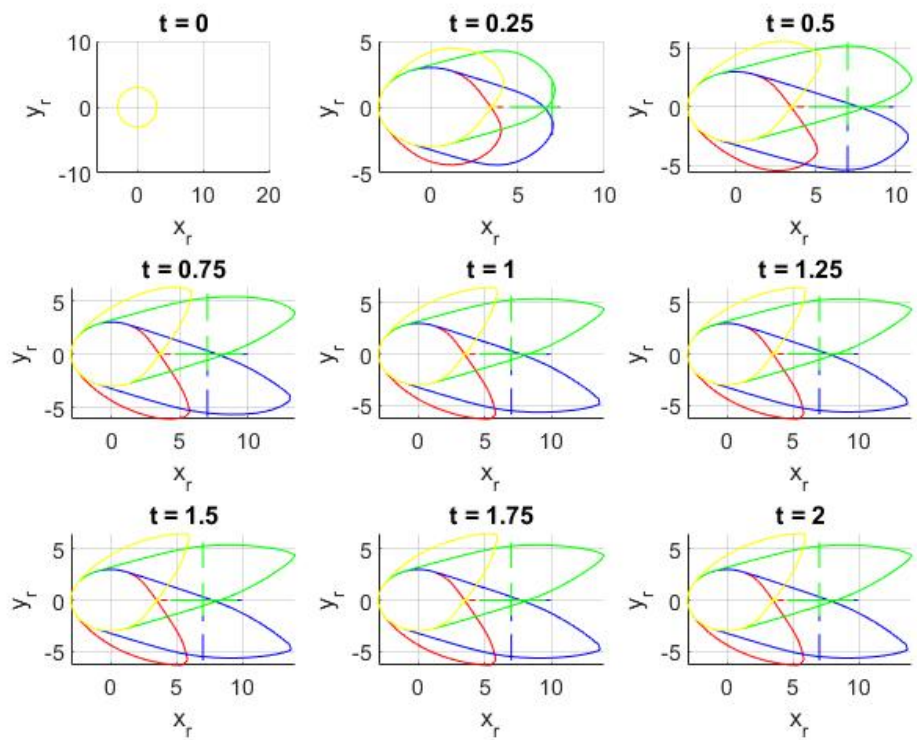


Fig. 7: 2D Contour Plot of Backward Reachable Set from  $t = -2$  to  $t = 0$

### C. One Evader and Four Pursuers (Different Speed ratio)

In this case, a different speed ratio was used with  $V_p = 7.5m/s$  which still satisfies the condition that  $\frac{V_p}{V_e} \geq \sin(\frac{180^\circ}{4})$ . Since the number of pursuers is the same, the range of values of  $\theta_{rj}$  does not change. As seen in figures 8 and 9, the obtained reachable set does not vary significantly from the results obtained in case B. However, based on the contour plots, it does appear that the size of the BRS has slightly decreased after decreasing the speed ratio.

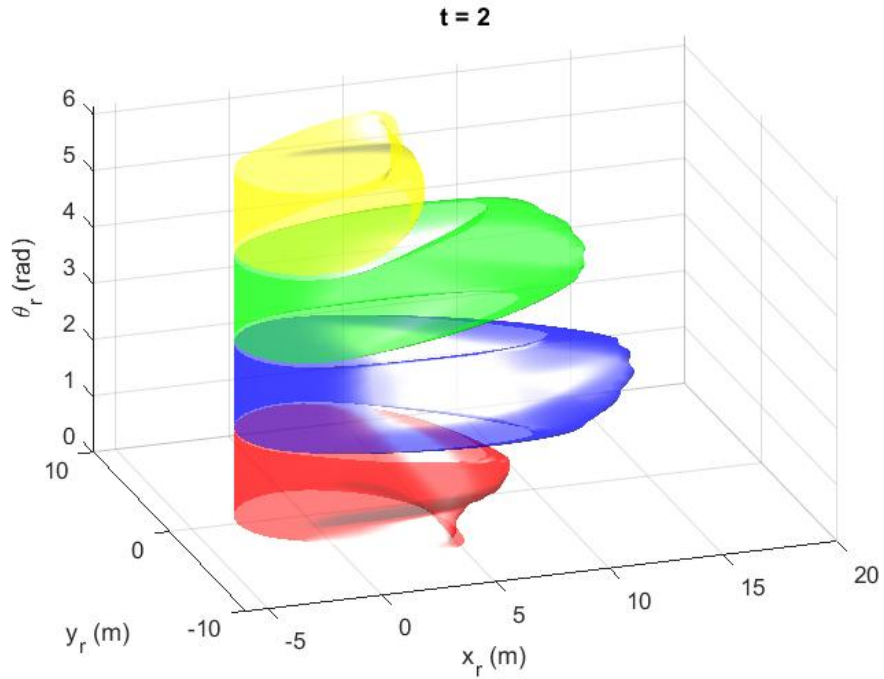


Fig. 8: Reachability Analysis for Four Pursuers and One Evader

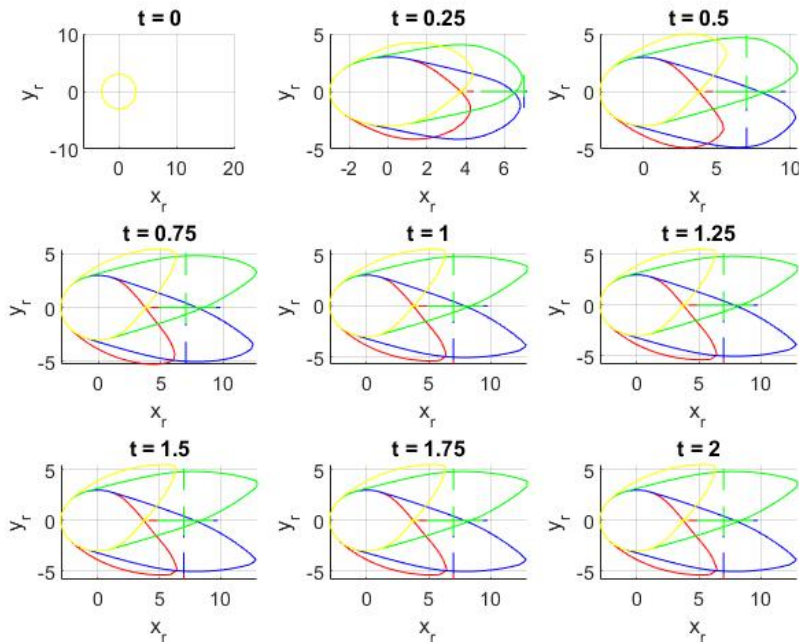


Fig. 9: 2D Contour Plot of Backward Reachable Set from  $t = -2$  to  $t = 0$

## V. CONCLUSION

From the previous discussion and the obtained results, it is clear how the computation of reachable sets can be beneficial in problems involving multi-player pursuit-evasion differential games in terms of achieving objectives like safety or attainability. By making use of system decomposition and the concept of the Apollonius circle, it was possible to perform reachability analysis for dynamic games involving inferior pursuers and the impact of the number of pursuers as well as the speed ratio on the backwards reachable set were investigated. Possible areas for further study in this domain would be cases involving more than 1 evader as well as the extension of the problem to 3 spatial dimensions, in order to consider scenarios involving aerial vehicles.

## CONTRIBUTIONS OF INDIVIDUAL MEMBERS

- **Apoorva Banerjee** proposed this topic, derived the first-order necessary conditions for the optimal control problem, and made an equal contribution in implementing the proposed methodology in the MATLAB Level Set Toolbox. He has also made a main contribution in preparing the presentation slides for this project, and has proofread this report.
- **Reuben Georgi** contributed in understanding and realizing concepts from the literature review, and has made an equal contribution in implementing the proposed methodology using the MATLAB Level Set Toolbox. Additionally, he has a main contribution in preparing this report.

## REFERENCES

- [1] Gillula, J. H., Hoffmann, G. H., Huang, H., Vitus, M. P., and Tomlin, C. J., "Applications of Hybrid Reachability Analysis to Robotic Aerial Vehicles," *The International Journal of Robotics Research*, Vol. 30, No. 3, 2011, pp. 335-354.
- [2] Altaher, M., Elmougy, S., and Nomir, O., "Intercepting a Superior Missile: A Reachability Analysis of an Apollonius Circle-based Multiplayer Differential Game," *International Journal of Innovative Computing Information and Control*, Vol. 15, No. 1, 2019, pp. 369-381.
- [3] Mitchell, I. M., "A Toolbox of Level Set Methods," *UBC Department of Computer Science Technical Report*, TR-2007-11, 2007
- [4] I. M. Mitchell, A. M. Bayen and C. J. Tomlin, "A time-dependent Hamilton-Jacobi formulation of reachable sets for continuous dynamic games," in *IEEE Transactions on Automatic Control*, vol. 50, no. 7, pp. 947-957, July 2005, doi: 10.1109/TAC.2005.851439.
- [5] Makkapati, Venkata Kothari, Mangal. (2017). Pursuit-Evasion Games of High Speed Evader. *Journal of Intelligent and Robotic Systems*. 85. 10.1007/s10846-016-0379-3.